Academic Journal of Emerging Technologies
ISSN Print: 3104-4417
ISSN Online: 3104-4425
CD ISSN: 3104-4433
https://doi.org/10.63313/AJET.9062

Multi-UAV Task Allocation Method for Road Emergency Rescue Based on Improved Multi-Objective Genetic Algorithm

Xiaoyu Wang*. Yangshan Tang and Ying Li
School of Automotive and Traffic Engineering, Liaoning University of Technology, Jinzhou 121000, China
Email: wxy18765693211@163.com

How to cite this paper: Wang, X., Tang, Y., & Li, Y. (2026). Multi-UAV Task Allocation Method for Road Emergency Rescue Based on Improved Multi-Objective Genetic Algorithm. Academic Journal of Emerging Technologies, 3(2), 1–10. ISSN Print: 3104-4417, ISSN Online: 3104-4425.
https://doi.org/10.63313/AJET.9062
Published: 2026-06-04

Copyright © 2026 by author(s) and Erytis Publishing Limited.
This work is licensed under the Creative Commons Attribution International License (CC BY 4.0).
http://creativecommons.org/licenses/by/4.0/

Abstract

To enhance the operational efficiency of multi-UAV material delivery in emergency rescue scenarios, this paper establishes a mathematical model for multi-UAV task allocation and proposes an improved hybrid multi-objective genetic algorithm, namely the AC-MOGA algorithm. Firstly, the multi-UAV material delivery task allocation problem is elaborated. A mathematical model is constructed with three optimization objectives: minimizing the total flight distance of UAVs, reducing the maximum task completion time, and optimizing the weighted total response time. Secondly, Logistic chaotic mapping and adaptive strategies are introduced to modify the multi-objective genetic algorithm. The improvements are implemented in population initialization, crossover and mutation operations to construct the proposed algorithm for problem solving. Finally, based on six groups of VRPLIB benchmark instances, numerical simulations are carried out on the MATLAB platform to obtain the task allocation schemes derived by the AC-MOGA algorithm. Comparative analyses with a state-of-the-art improved genetic algorithm are conducted on identical benchmark instances. The results verify the effectiveness and feasibility of the AC-MOGA algorithm for solving vehicle routing problems.

Keywords

UAV; Emergency Rescue; Task Allocation; Multi-objective Genetic Algorithm; Capacitated Vehicle Routing Problem

1. Introduction

Road emergency rescue is a complex and time-sensitive task. Multiple factors need to be taken into comprehensive consideration to ensure the rescue operations are carried out efficiently, safely and in an orderly manner, so as to minimize casualties and property losses.Its core research mainly focuses on two aspects: establishing task allocation models and designing appropriate algorithms for model solving. In

Reference [1], taking average waiting time and flight distance as evaluation indicators for task allocation schemes, a constrained optimization model was constructed by adopting penalty functions to handle multiple constraints. In Reference [2], considering UAV load capacity, flight range and task collaboration, a cost optimization model was established with the minimum operational loss and maximum task benefit as objectives. In Reference [3], accounting for the time cost of different UAVs, the problem was abstracted into an extended Team Orientation Problem (TOP), and a corresponding extended TOP model was built.

Corresponding algorithms need to be developed to solve the established task allocation models. Reference [4] adopted an adaptive genetic algorithm (AGA) integrating the roulette wheel selection and elitist preservation strategies for model solving, which accelerated the convergence rate and improved optimization performance.Reference [5] put forward a distributed auction algorithm and introduced a coalition competition equilibrium mechanism to address the challenges arising from task execution by multi-robot coalitions. Reference [6] developed an improved marine predators algorithm (LGMPA) integrated with the logarithmic spiral strategy and Gaussian distribution estimation strategy to avoid local optima.By introducing a parallel mechanism, Reference [7] proposed the PMOGWO algorithm, which strengthens the ability to escape local optima and speeds up the optimization process. Reference [8] designed a hybrid optimization algorithm based on the improved NSGA-III algorithm to boost solution accuracy. Reference [9] presented a multi-UAV task planning algorithm based on evolutionary multitasking, achieving higher search efficiency.Therefore, this paper constructs a multi-UAV task allocation model according to practical rescue scenarios, and adopts a multi-objective genetic optimization algorithm to solve the model. On the basis of the traditional multi-objective genetic algorithm, relevant improvements are made, and simulation experiments are carried out to verify the effectiveness of the improved algorithm.

2. Multi-UAV Task Allocation Model for Road Emergency Rescue

2.1. Problem Description

This paper formulates the task allocation problem of multi-UAV road emergency rescue as follows. It is assumed that a major accident triggering multiple secondary incidents has occurred on a mountain road. The emergency rescue center needs to dispatch multiple UAVs to deliver supplies to several accident sites. Each site requires food, first-aid supplies, safety equipment and other materials, which are packaged into integrated supply parcels to be airdropped by UAVs. The location of all accident sites is known in advance. All UAVs depart from the same emergency rescue center and must return to the base station after completing assigned tasks. Subject to various constraints, the objective is to minimize the energy consumption of the UAV swarm and accomplish rescue missions rapidly and efficiently.

2.2. Parameter Description

For the convenience of subsequent description of the task allocation problem, the relevant variables of the proposed model are defined in Table 1.

Table 1. Parameter description

Notations	Description
N	Total number of UAVs, $k(k=1,2,\cdots,N)$: UAV index
M	Total accident sites, $i,j(i,j=1,2,\cdots,M)$: accident site indices
d_{ij}	U_k distance from accident site i to site j
v_k	U_k speed of UAV (maximum cruising speed of UAV)
t_{ij}	U_k time from accident site i to site j
T_k	Total time for a U_k to complete rescue tasks
τ_i	Airdrop time at accident site i
x_{ij}^k	Decision variables, U_k travels from accident site i to site j, x_{ij}^k =1, Conversely, x_{ij}^k =0
y_i^k	Decision variables, The U_k delivers supply packages to accident site i, y_i^k =1, Conversely, y_i^k =0
$W_{\max}$	Maximum carrying capacity of supplies for UAV
w_i	Supply demand at accident site i
ω_j	Priority weight of accident site j
α_j	Total time for U_k to arrive at and complete delivery at accident site j
$T_{\max}$	Maximum flight endurance of the UAV

2.3. Parameter Description

Suppose $U=\{U_1,U_2,\cdots,U_N\}$ stands for the UAV. The number of UAVs is N. The total number of accident sites is M, represented by $T=\{T_1,T_2,\ldots,T_M\}$. Let each UAV fly at a constant speed, and each accident site can be visited only once. The model aims to minimize the weighted response time, the total task completion time and the total flight distance.

Minimize the total weighted response time f_1, as shown in Equation (1).

$$f_1=\sum_{j=1}^{M}\omega_j a_j \tag{1}$$

$$\alpha_j=t_{ij}+\tau_j \tag{2}$$

Minimize the maximum task completion time f_2, as shown in Equation (3).

$$f_2=Max\{T_k\} \tag{3}$$

where the flight time of the UAV traveling from accident site i to another site j is

expressed by Equation (4), and the total time for a UAV to complete multiple rescue tasks is given by Equation (5).

$$t_{ij} = \frac{d_{ij}}{v_k} \tag{4}$$

$$T_k = \sum_{i=1}^{N}\sum_{j=0}^{N} x_{ij}^k t_{ij} + \sum_{i=1}^{N} \tau_i y_i^k \tag{5}$$

Minimize the total flight distance f_3, as shown in Equation (6).

$$f_3 = \sum_{k=1}^{N}\sum_{i=0}^{M}\sum_{j=0}^{M} x_{ij}^k d_{ij} \left(i \neq j\right) \tag{6}$$

Combined with the practical characteristics of the multi-UAV task allocation for road rescue and the inherent performance requirements of UAVs, the following constraints are established to guarantee the feasibility and efficiency of task execution.

The constraint that each accident site is visited by exactly one UAV for only once is shown in Equation (7).

$$\sum_{k=1}^{N} y_i^k = 1, \quad \forall i = 1,2,\cdots,M \tag{7}$$

The maximum battery life constraint is given by Equation (8):

$$T_k \leq T_{\max} \tag{8}$$

The constraints on central cities are given by Equation (9):

$$\sum_{j=0}^{M} x_{0j}^k = \sum_{i=0}^{M} x_{i0}^k, \quad \forall k = 1,2,\cdots,N \tag{9}$$

The maximum load constraint is given by Equation (10):

$$\sum_{i=1}^{M} w_i y_i^k \leq W_{\max}, \quad \forall k = 1,2,\cdots,N \tag{10}$$

Finally, a multi-drone road rescue mission allocation model was developed with objective functions minimizing the weighted total response time, the maximum task completion time, and the total flight distance, as shown in Equation (11):

$$\begin{aligned} & F = \min\left\{f_1, f_2, f_3\right\} \\ & s.t. \sum_{k=1}^{N} y_i^k = 1, \forall i = 1,2,\cdots,M \\ & \sum_{j=0}^{M} x_{0j}^k = \sum_{i=0}^{M} x_{i0}^k, \forall k = 1,2,\cdots,N \\ & \sum_{i=1}^{M} w_i y_i^k \leq W_{\max}, \forall k = 1,2,\cdots,N \\ & T_k \leq T_{\max} \end{aligned} \tag{11}$$

3. Task allocation solution based on the AC-MOGA algorithm

(1) Chromosomal encoding and decoding

This paper employs integer encoding to represent chromosomes and adopts a dual-chromosome structure to clearly distinguish between drone allocation schemes and task sequences, thereby avoiding decoding ambiguities caused by encoding coupling—specifically, the issue of high-quality sequence assignments being mapped to suboptimal task allocations during optimization. The two chromosomes represent the set of accident points to be visited (chromosome I) and the set of segmentation points that divide chromosome I into multiple gene segments; each gene segment corresponds to a sequence of accident points sequentially visited by a drone (chromosome II). The set of segmentation points generated by chromosome II serves as the position indices for chromosome I (denoted as p), By splitting after the i-th element of chromosome I, the task allocation scheme for the drone is obtained.

(2)Population Initialization

Our study employs a hybrid initialization strategy combining the Logistic chaotic mapping from discrete chaos systems and stochastic greedy nearest neighbor optimization under constraint constraints. Exploration individuals generate customer visit sequences (chromosome 1) using Logistic chaotic mapping and develop drone task segmentation plans (chromosome 2) through constrained perturbation mechanisms, maximizing solution diversity while maintaining feasibility. Optimization individuals similarly utilize chaotic mapping to establish initial visit sequences and apply stochastic greedy nearest neighbor optimization to each task segment while adhering to constraints, thereby enhancing initial solution quality. To prevent premature convergence, constraint parameters are subject to ±10% random perturbations during initialization, and greedy optimization selects nearest customers with only 80% probability while directly retaining chaotic-generated sequences in 20% cases.

The logistic chaotic mapping's mathematical expression is given in Equation (12):

$$x_{i+1} = a x_i \left(1 - x_i\right), \quad a \in \left(0, 4\right] \tag{12}$$

Here, α = 4 (full chaotic state), with the chaotic orbit state values ranging from (0, 1).

Adaptive Cross-Variation Strategy.

① Individual fitness assessment

For individuals in a population with Rank=1, set the fitness value of the individual with the highest crowding distance (CD) to 1 and that of the second-highest CD to 2; apply this method to assign fitness values to all individuals at this level. Repeat the Rank1 approach to assign fitness values to all individuals across all levels. To prevent evaluation failures due to magnitude differences, standardize the fitness values first using Formula (13).

$$F_{norm}\left(i\right) = \frac{F\left(i\right) - F_{\min}}{F_{\max} - F_{\min}} \tag{13}$$

Here, $F_{norm}\left(i\right)$ is the standardized fitness value; $F\left(i\right)$ is the comprehensive quality

index of individual i; $F_{\min}$ and $F_{\max}$ are the minimum and maximum fitness values in the population.

② Determination of the Relative Benchmark

$$F_{base} = F_{norm} \cdot p \tag{14}$$

Among them, F_{base} as the population benchmark point to distinguish between superior and inferior indi viduals; the control parameter p is set to 0.6.

The mathematical formulas for the baseline crossover probability $p_{c,base}$ and baseline variation probability $p_{m,base}$ are given in Equations (15) and (16), respectively:

$$p_{c,base} = \frac{p_{c,\max} + p_{c,\min}}{2} \tag{15}$$

$$p_{m,base} = \frac{p_{m,\max} + p_{m,\min}}{2} \tag{16}$$

Among them, and represent the maximum and minimum cross probabilities, with values of 0.6 and 0.9, respectively; and represent the maximum and minimum variation probabilities, with values of 0.01 and 0.1, respectively.

③ Segmental relative benchmark calculation

Upper region (high-quality) $relative_pos_{upper}(i)$ indicates the relative strengths and weaknesses of high-quality individuals:

$$\text{relative_pos}_{upper}(i) = \frac{F_{norm}(i) - F_{base}}{1 - F_{base}} \tag{17}$$

Lower region (inferior quality) $relative_pos_{lower}(i)$ indicates the relative merits and inferiorities of poor individual i:

$$\text{relative_pos}_{lower}(i) = \frac{F_{lower} - F_{norm}(i)}{F_{base}} \tag{18}$$

Sigmoid function:

$$S(x) = \frac{1}{1 + e^{-k(x-0.5)}} \tag{19}$$

Here, $S(x)$ is the Sigmoid function; k is the steepness factor to control the steepness of the curve; x is the input value.

The formula for calculating the adaptive probability of crossover and variation is shown in formulas (20)-(23) below.

For individuals in the upper half of the region($F_{norm}(i) \geq F_{base}$):

$$p_c(i) = p_{c,base} + (p_{c,\max} - p_{c,base}) \cdot S\left(relative_pos_{upper}(i)\right) \tag{20}$$

$$p_m(i) = p_{c,base} - (p_{m,base} - p_{m,\min}) \cdot S\left(relative_pos_{upper}(i)\right) \tag{21}$$

For individuals in the lower half of the area ($F_{norm}(i) < F_{base}$):

$$p_c(i) = p_{c,base} - (p_{c,\ \text{base}} - p_{c,\min}) \cdot S\left(1 - relative_pos_{\text{lower}}(i)\right) \tag{22}$$

$$p_m(i) = p_{c,base} + (p_{m,\max} - p_{m,base}) \cdot S\left(1 - relative_pos_{lower}(i)\right) \quad (23)$$

The adaptive crossover variation strategy dynamically adjusts t he intensity of genetic operations to effectively balance the algorithm's exploration and development capabilities. It dynamically modifies the crossover and mutation rates based on the population's evolutionary state (e.g., individual fitness, distribution density) to enhance exploration during early evolution or when population diversity is low, thereby facilitating global search; and to strengthen development in later stages or near optimal regions, accelerating fine-tuned convergence.

(4)Improved elite retention strategy for external archiving and population merging

To enhance algorithmic convergence while preserving the distributive nature of the Pareto front, this algorithm introduces an improved mechanism based on external archiving and population merging, building upon the standard elite retention strategy. The implementation process comprises the following steps:

①Initialization: Create an initial population and initialize an empty external archive to store high-quality solutions during the iteration process.

② Evolutionary Cycle (for Generation):

1) After initialization, the population generates offspring populations from the current population through computations using genetic operators such as selection, crossover, and mutation.

2) Merge populations: Combine the parent population, offspring population, and external archive to form a combined population.

3) Non-dominated sorting: Perform rapid non-dominated sorting on all individuals in the set and divide them into several non-dominated layers.

4) Population Construction and Archive Updates: Starting from the highest non-dominated layer, add individuals sequentially to the next-generation population and new external archives until reaching a layer where the total size exceeds the threshold. For each layer, calculate the crowding distance of its individuals and select them in descending order of crowding value to fill the remaining capacity in both the population and archives.

5) Archive Maintenance: If the size of the external archive A i+1 exceeds the preset maximum value, pruning is performed to remove individuals from the most densely distributed regions, ensuring optimal archive size and distribution.

③End when the termination condition is met.

4. Simulation Experiment

In this experiment, the two-dimensional coordinates of each city or node in the CVRPLIB dataset are used to represent the locations of accident points on roads.To simplify problem-solving, all drones operate under identical flight conditions with a endurance of 300 minutes, an average flight speed of 20 m/s, and no velocity variations during takeoff or landing phases.

Based on four experimental instances from the CVRPLIB dataset, the proposed AC-MOGA algorithm was employed to solve the multi-drone task assignment problem and generate corresponding solutions. The algorithm parameters were optimized to balance convergence efficiency and population diversity: a population size of 100, a maximum number of iterations of 200, an adaptive crossover probability with a dynamic range of [0.6, 1], and an adaptive mutation probability within the range [0.05,0.2]. This parameter configuration enables the algorithm to effectively balance global exploration and local optimization during evolution. The final simulation results are summarized in Table 2.

Table 2. Simulation results

Example	Number of accident points per item	Running time per second	Mission sequence
A-n32-k5	32	6.429	UAV 1：2-3-4-29-5-16-20 UAV 2：28-8-11-9-15-10 UAV 3：13-6-18-22-25-24 UAV 4：7-21-31-19-17-23 UAV 5：30-26-12-1-16-14-27
A-n38-k5	38	6.378	UAV 1：14-15-17-18-34-16-19 UAV 2：9-3-4-37-11-7-31 UAV 3：29-12-1-23-35-36-13-2 UAV 4：5-25-26-21-10-20-24 UAV 5：33-8-30-6-28-27-22-32
B-n45-k5	45	8.541	UAV 1：15-13-6-17-23-12-1-26-38-45 UAV 2：25-4-16-34-5-37-2-40-43 UAV 3：22-11-27-28-6-30-39-44 UAV 4：32-7-31-18-10-3-8-9-41-42 UAV 5：33-35-29-19-21-20-24-14
B-n39-k5	39	7.001	UAV 1：8-23-35-1-16-3-24 UAV 2：14-13-17-36-5-28-11 UAV 3：9-21-18-6-31-37-26-32 UAV 4：33-12-29-10-30-20-25-19-38 UAV 5：34-4-7-22-27-15-2-39

Figure 1 illustrates the optimization results for distinct scenarios, corresponding to path allocation schemes associated with three single-objective optimal solutions: minimizing weighted total response time (f_1), minimizing maximum task completion time (f_2), and minimizing total flight distance (f_3). Since multi-objective optimization does not seek a single global optimum but rather generates a set of Pareto-optimal solutions that balance multiple objectives, decision-makers can select the most suitable allocation scheme based on their specific preferences and priorities.

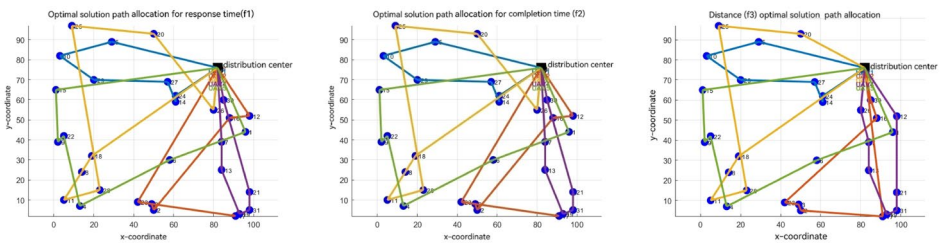


Figure 1. The optimal solution for different objective functions

To verify the algorithm's effectiveness, the improved multi-objective genetic algorithm (AC-MOGA) was simulated and compared with the original multi-objective genetic algorithm (MOGA) and the improved reference-point-based

non-dominated sorting genetic algorithm (ABCSA-NSGA) described in reference [11]. All experiments used an initial population size of 100 individuals and a maximum iteration count of 200; the simulation results are presented in Table 3.

Table 3. Data simulation results from three different algorithms

Example	Accident points: per case	Algorithm name	F1 optimal solution	F2 Optimal solution per minute	F3 optimal solution per km	Running time per second
A-n32-k5	32	AC-MOGA	736.300	36	154.654	6.429
		NSGA-II	779.985	41	164.268	8.716
		ABCSA-NSGA	796.215	39	156.624	6.319
A-n38-k5	38	AC-MOGA	748.784	34	114.921	6.378
		NSGA-II	810.354	37	156.336	8.542
		ABCSA-NSGA	854.236	48	146.554	8.556
B-n45-k5	45	AC-MOGA	841.562	43	198.596	8.541
		NSGA-II	874.562	52	221.578	10.254
		ABCSA-NSGA	914.325	51	217.653	9.264
B-n39-k5	39	AC-MOGA	818.674	37	156.319	7.001
		NSGA-II	912.647	44	174.586	8.264
		ABCSA-NSGA	894.135	40	166.853	9.561

Analysis of the simulation results in Table 3 reveals that the original multi-objective genetic algorithm exhibits significant shortcomings in both solution quality and computational efficiency, performing markedly worse than the improved reference-point-based non-dominated sorting genetic algorithm and the proposed enhanced multi-objective genetic algorithm. Particularly regarding objective function values, our algorithm produces solution sets closer to the true Pareto front, demonstrating clear advantages in both convergence speed and solution distribution. Additionally, it demonstrates faster convergence rates and lower computational time, indicating superior engineering applicability while maintaining high solution quality.

5. Conclusions

This article proposes an improved genetic algorithm framework for emergency supplies transportation scenarios. Core improvements to this framework include: adopting a two-chromosome coding structure to represent task sequences and resource allocation relationships separately, thereby clearly decoupling the two types of decision variables; Cross, mutation, and selection operators adapted to these conditions were designed to balance convergence efficiency and population diversity; The Logistic chaotic mapping method is introduced for population initialization, enhancing the quality and uniformity of the initial solution, laying a solid foundation for algorithm search. Finally, comparative experiments with other classical and improved genetic algorithms verify the superiority and effectiveness of the proposed method from multiple aspects such as convergence speed, solution quality, and stability.

References

[1] Zhang X Y, Xia S, Zhang T. Multi-UAV cooperative task allocation based on adaptive

genetic learning particle swarm algorithm. Control and Decision, 2023, 38(11): 3103-3111.

[2] Yuan T B. Research on Task Pre-allocation and Re-allocation Technology for Heterogeneous Multi-UAV Cooperative Combat [D]. University of Electronic Science and Technology of China, 2024.

[3] Zhao Y. Research on Multi-UAV Cooperative Task Allocation and Path Planning Technology [D]. University of Electronic Science and Technology of China, 2022.

[4] Xiong T, Liu F, Liu H, Ge J, Li H, Ding K, Li Q. Multi-Drone Optimal Mission Assignment and 3D Path Planning for Disaster Rescue. Drones. 2023; 7(6):394.

[5] DENG R L, YAN R, HUANG P N, et al. A Distributed Auction Algorithm for Task Assignment With Robot Coalitions[J]. IEEE Transactions on Robotics, 2024, 40(4): 4787-4804.

[6] Zhang Z R, Cheng H, Han B, et al. Multi-UAV cooperative task assignment method based on LGMPA algorithm [J]. Modern Electronics Technique, 2025, 48(04): 109-118.

[7] Wang Z, Hua X. Multi-UAV task assignment based on improved multi-objective grey wolf optimization algorithm [J]. Journal of Xi'an Technological University, 2021, 41(01): 94-102.

[8] Wang S Y, Shen Q M, Sun M Y, et al. Multi-UAV cooperative target allocation based on improved NSGA-III algorithm [J]. Aero Weaponry, 2024, 31(04): 100-111.

[9] Ma H J, Sun B, Zhang W. Multi-AUV cooperative task allocation based on improved bee colony algorithm [J]. Control Engineering, 2024, 12(17): 1-7.